

## Stochastic well capture zones in fully, leaky, and randomly confined, heterogeneous aquifers

**MATTHIJS VAN LEEUWEN, ADRIAN P. BUTLER,  
JACOB A. TOMPKINS**

*Department of Civil and Environmental Engineering, Imperial College of Science, Technology and Medicine, Imperial College Road, London SW7 2BU, UK*

e-mail: [m.vanleeuwen@ic.ac.uk](mailto:m.vanleeuwen@ic.ac.uk)

**CHRIS B. M. TE STROET**

*Faculty of Civil Engineering, Delft University of Technology, Stevinweg 1, 2628 CN Delft, The Netherlands*

**Abstract** A stochastic approach is adopted for characterizing the uncertainty in well capture zones due to heterogeneity. Three different levels of aquifer confinement are considered: (a) a fully confined and (b) a leaky-confined aquifer in which the transmissivity of the aquifer is modelled as a random space function; and (c) a randomly confined aquifer in which both the transmissivity of the aquifer and the conductance of an overlying clay cover are modelled as random space functions. A Monte Carlo approach is used to infer the probability distribution of the resulting stochastic capture zones.

### INTRODUCTION

The accurate determination of well capture zones is of great importance, not only from an environmental point of view, but also in terms of public health. The location of a capture zone depends to a large extent on the hydrogeological properties of the production aquifer and adjacent layers. The uncertainty that stems from the heterogeneity of the hydrogeological properties calls for a stochastic approach in which one or more properties are modelled as a random space function (RSF). Of the hydraulic properties relevant to capture zones, the transmissivity of the production aquifer,  $T$  [ $L^2 T^{-1}$ ], and the conductance,  $c$  [ $L T^{-1}$ ], of overlying layers such as clay covers are considered to be of major importance as their variability in space is considerably higher than that of other relevant properties.

The (spatial) stochastic approach enables the capture zone to be presented using areas of confidence, rather than a single zone with an unquantified uncertainty. An additional advantage of the spatial stochastic approach is its optimal use of available spatial data by not only considering these values, but also their spatial attributes (location and correlation structure). This facilitates a realistic representation of natural variability and, because it optimizes the use of available data, does not produce unsupported overly conservative estimates of uncertainty. When applied to capture zone delineation, the stochastic approach results in a stochastic capture zone, the probability distribution of which is referred to as the capture zone probability distribution (capd). The capd gives the spatial distribution of the probability,  $P[x,t]$ , that a conservative tracer particle released at a particular location,  $x$ , is captured by the well within a certain time duration,  $t$ .

The theoretical and practical aspects of the stochastic determination of capture zones have been dealt with by several authors (Varljen & Shafer, 1991; Franzetti & Guadagnini, 1996; Guadagnini & Franzetti, 1999; Van Leeuwen *et al.*, 1998). A case study in which capture zones are determined stochastically using random space functions has been carried out by Van Leeuwen *et al.* (1999).

In the present paper, capture zone probability distributions (capds) are studied in three heterogeneous aquifers with different level of confinement: (a) a fully-confined aquifer, (b) a leaky-confined aquifer, and (c) a randomly confined aquifer.

## FULLY- AND LEAKY-CONFINED HETEROGENEOUS AQUIFERS

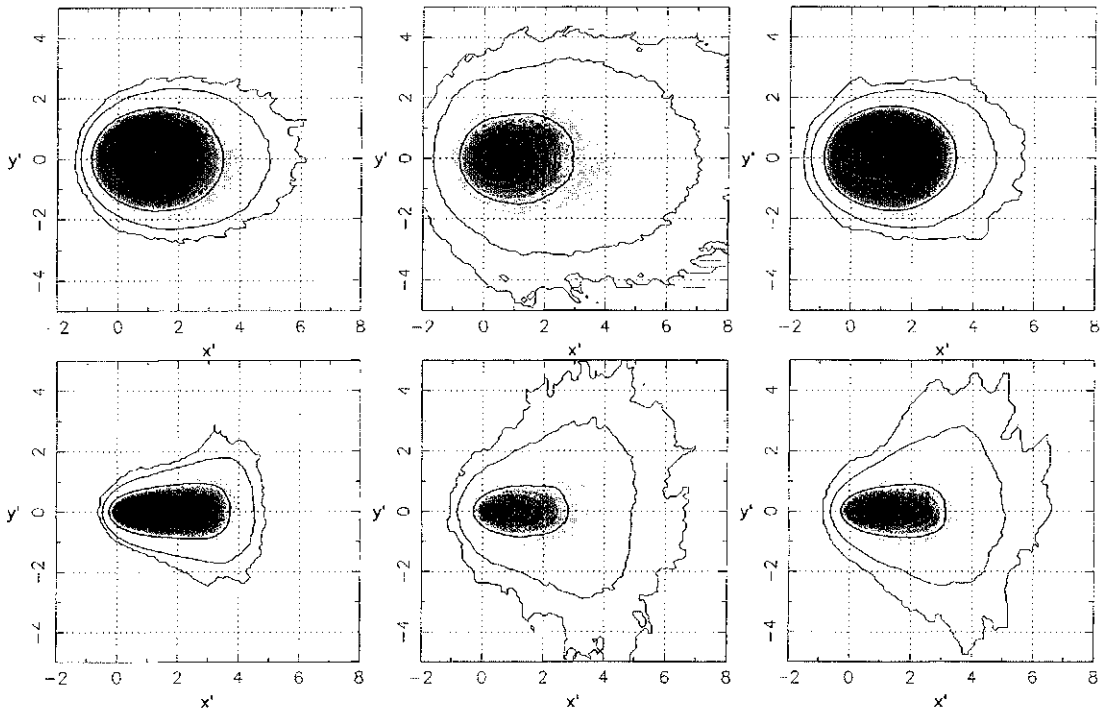
### Numerical approach

In this section, we consider a fully confined aquifer with a mean uniform background gradient  $\mathbf{J} = (J, 0)$ . A fully penetrating well—or, more strictly, wellfield at this scale—is pumping with a constant discharge per unit aquifer thickness,  $Q$  [ $L^2 T^{-1}$ ]. Its size in the model is equal to one grid cell and its centre is at the origin of a Cartesian coordinate system  $\mathbf{x} = (0, 0)$ . Results will be presented using the following dimensionless coordinates:  $x' = (2\pi q_0/Q)x$ ,  $y' = (2\pi q_0/Q)y$ ,  $t' = (2\pi q_0^2/nQ)t$ , where  $q_0 = \bar{T}_G J$  [ $L T^{-1}$ ] is the Darcy background flow velocity,  $\bar{T}_G$  [ $L T^{-1}$ ] is the geometric mean transmissivity  $T_G$  per unit aquifer thickness, and  $n$  is the effective porosity. In the leaky-confined case, a combination of recharge and drainage is applied which results in a water mound with a water divide at  $x' \approx 4.5$ . Transmissivity  $T$  is assumed to be lognormal distributed and its fluctuation  $Y = \ln(T/T_G)$  is regarded as an isotropic, stationary, multi-Gaussian RSF with zero mean. The two-point covariance of  $Y$  is given by  $C_Y(\mathbf{h}) = \sigma_Y^2 \exp(-|\mathbf{h}|/I_Y)$ , where  $\mathbf{h}$  is the lag separation vector,  $I_Y$  is the integral scale and  $\sigma_Y^2$  is the variance. The integral scale is made dimensionless using  $I'_Y = (2I_Y\pi q_0)/Q$ .

Numerical estimates of  $P[\mathbf{x}, t']$  are obtained through Monte Carlo (MC) analyses, each comprising a total of 1000 realizations. For each MC realization, a realization of  $T$  is generated and used in a deterministic capture zone delineation using forward particle tracking. The ensemble of realizations is treated statistically in order to infer the capd. The boundaries of the numerical model are positioned sufficiently far from the capture zone as to minimize their effect on the numerical solution. A grid node size of  $\Delta x' = 0.1$  is chosen for all simulations.

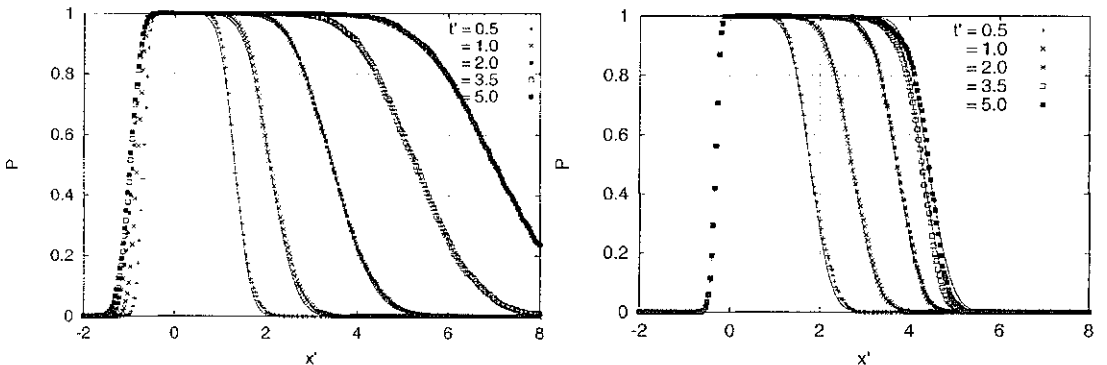
### Results and discussion

Figure 1 shows contour plots of  $P[\mathbf{x}', t']$  for different values of  $\sigma_Y^2$  and  $I'_Y$ , for both aquifer models. It can be seen how uncertainty in  $T(\mathbf{x}')$  results in uncertainty in the boundaries of the capture zone and how an increase in  $\sigma_Y^2$  results in an expansion of the zone of uncertainty ( $0 < P < 1$ ). The influence of  $I'_Y$  is hardly noticeable in the fully confined case for the  $I'_Y = 0.5$  and  $I'_Y = 5$  shown here, but the insensitivity was also found for larger integral scales. In the leaky-confined case, an increase in  $I'_Y$  results in an expansion of the zone of uncertainty.



**Fig. 1** Contour plots of the cpd for different values of  $P_Y$  and  $\sigma_Y^2$  in the fully confined case (top row) and the leaky-confined case (bottom row). Grey scales from  $P = 0$  (white) to  $P = 1$  (darkest grey). Left:  $P_Y = 0.5$ ,  $\sigma_Y^2 = 0.5$ , middle:  $P_Y = 5$ ,  $\sigma_Y^2 = 3$ , right:  $P_Y = 5$ ,  $\sigma_Y^2 = 0.5$ . For all:  $t' = 2$ .

Figure 2 shows plots of  $P[\mathbf{x}', t']$  along the  $x'$ -axis ( $y' = 0$ ) and the  $y'$ -axis ( $x' = 0$ ) for different times  $t'$ . The excellent match in Fig. 2 between the numerical results indicated by the markers, and the theoretical cumulative normal distributions indicated by the full lines, suggests that  $P(x' > 0, y' = 0)$  is normally distributed. In both the fully confined and the leaky-confined case, the distributions depart from normality when  $\sigma_Y^2$  or  $P_Y$  increase.



**Fig. 2** Graphs of the cpd along the  $x'$ -axis in the fully-confined case (left) and the leaky-confined case (right) for different  $t'$ . The full lines represent theoretical cumulative normal distributions. For both:  $P_Y = 0.5$ ,  $\sigma_Y^2 = 0.5$ .

A clear difference between the cases is the behaviour of the capds in time (Fig. 2). In the fully confined case, the curves do not just move along the axes, but the uncertainty increases too. This is due to the fact that the released particles travel longer and encounter more heterogeneity as the capture zone expands with time. In the leaky-confined case, the uncertainty increases initially, but when the capd reaches the water mound at  $x' \approx 4.5$  its expansion is inhibited and the uncertainty decreases again.

## RANDOMLY CONFINED HETEROGENEOUS AQUIFER

This section describes a case study in which capture zone probability distributions (capds) are determined for a well field pumping from a heterogeneous aquifer which is covered by a very heterogeneous clay layer. The well field is located near the town of Wierden in the east of The Netherlands.

The aquifer system comprises two main aquifers (Fig. 3, left). The upper aquifer is overlain by a top system which mainly consists of a continuous layer of very fine sands. The lower aquifer is divided into a lower part with fine sands and an upper part with coarse sands. A very heterogeneous clay layer, with many discontinuities and a spatially highly variable thickness, separates the upper and lower aquifers in places. There are several abstractions for drinking water supply and industrial purposes in the area, the well screens of which are located in the upper part of the lower aquifer.

An existing, comprehensively calibrated, numerical groundwater flow model was used: the Wierden model (Hoogendoorn & Te Stroet, 1994; Te Stroet, 1995). This deterministic model describes an area of  $22 \times 22$  km and uses a numerical grid comprising 99 columns and 98 rows. The grid spacing varies from 125 m to 1 km.

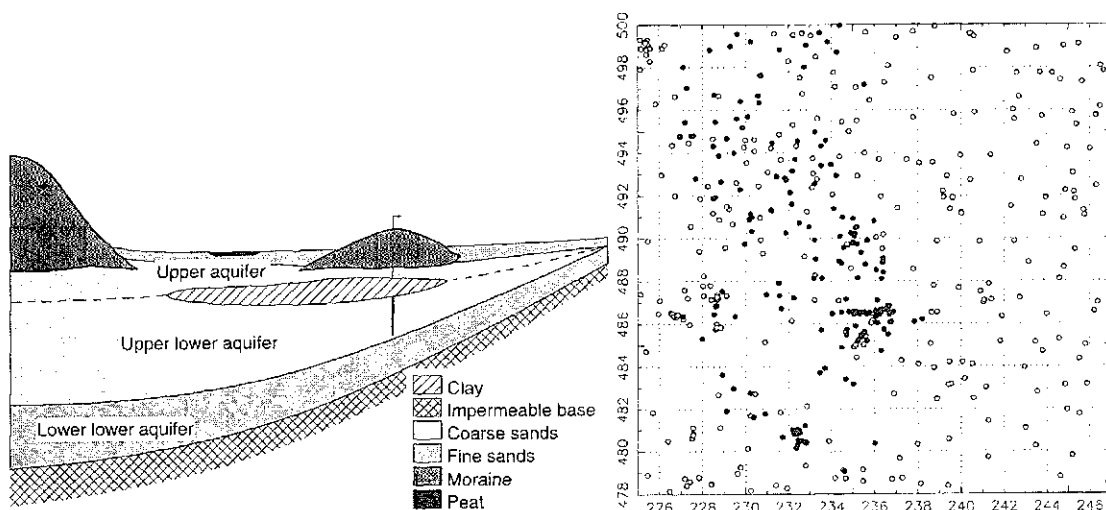


Fig. 3 Vertical hydrogeological conceptualization (left) and map of borehole locations in the model domain (right). The full circles in the map indicate boreholes where clay was encountered, the open circles where no clay was encountered.

### Analysis of the clay layer

The structural analysis of the clay layer is based on a set of 1643 borehole descriptions, selected from the REGIS (Regional Geohydrologic Information System) database (Broers *et al.*, 1994). The borehole descriptions pertain to boreholes located within the model domain plus an extra zone of 10 km outside the domain. The number of boreholes within the model domain is 546, 235 of which encountered clay. Figure 3 (right) shows the locations of the selected borcholes within the model domain.

The clay layer is described using two dependent variables: (a) a binary variable  $d_{\text{bin}}(\mathbf{x})$  describing its presence, and (b) a continuous variable  $d(\mathbf{x})$  describing its thickness. At each borehole location,  $d_{\text{bin}}$  is assigned the value 1 if clay is present or the value 0 if not. At each location where clay was encountered and the borehole is deep enough to measure both top and bottom of the clay layer,  $d$  exists and is assigned the measured thickness. The indicator semivariogram pertaining to  $d_{\text{bin}}$  shows a low nugget which implies a high correlation at short distances. The distance over which the variable remains correlated (the range) is approximately a quarter of the domain length. The experimental semivariogram pertaining to  $d$  exhibits little correlation, both at short and long distances, and the range almost equals the domain length. The histogram of  $d$  suggests that the clay thickness tends to a lognormal distribution.

### Stochastic clay conductance and transmissivity models

In a stochastic model of the clay layer, both  $d_{\text{bin}}$  and  $d$  are modelled as an RSF and simulated using conditional stochastic indicator simulation and conditional sequential Gaussian simulation respectively. The resulting fields are combined into a new field by replacing all values of 1 in the field  $d_{\text{bin}}(\mathbf{x})$  by the corresponding value of  $d(\mathbf{x})$ . The thickness values are translated into conductance values according to  $c(\mathbf{x}) = 0.001/d(\mathbf{x})$  if  $d_{\text{bin}}(\mathbf{x}) = 1$ , and  $c(\mathbf{x}) = 0.5$  if  $d_{\text{bin}}(\mathbf{x}) = 0$ . Figure 4 shows maps of one realization of both types of simulation, as well as the combined map.

The transmissivity values in the original Wierden model were obtained by multiplying the spatially distributed aquifer thickness by a homogeneous value of

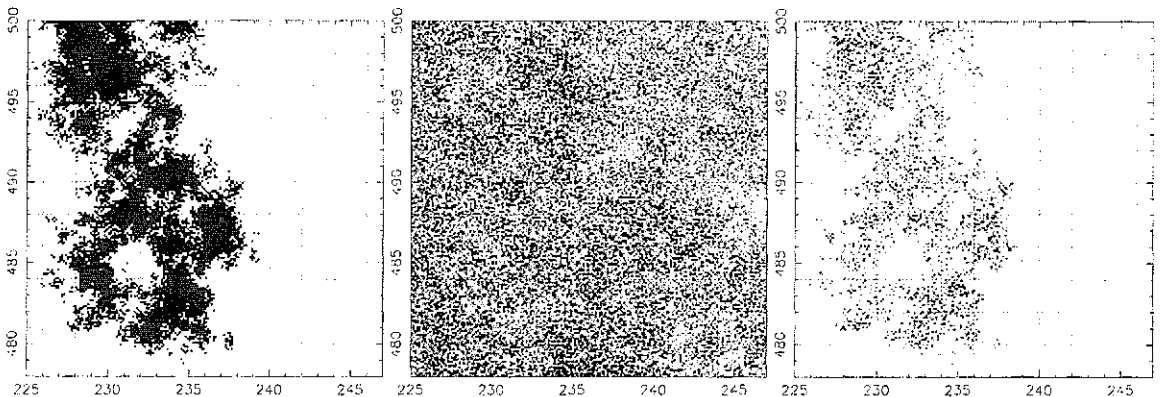


**Fig. 4** Image maps of the stochastic clay layer model. Left:  $d_{\text{bin}}$ , middle:  $d$ , right:  $c(\mathbf{x})$ . (Coordinates in km National Grid reference.)

hydraulic conductivity. In the stochastic approach used here, the hydraulic conductivity of the production aquifer has been modelled as an isotropic, normally distributed, random space function  $Y = \ln K$  with a mean value equal to the natural logarithm of the homogeneous conductivity. The stochastic properties of the function, such as its variance and correlation length, are unknown and no measurements are available to estimate them. On the basis of qualitative knowledge about the deposit and values reported in literature (e.g. Hoeksema & Kitanidis, 1985), an exponential two-point covariance model  $C_Y(\mathbf{h}) = \sigma_Y^2 \exp(-|\mathbf{h}|/I_Y)$  was adopted, where  $\mathbf{h}$  is the lag separation vector, the integral scale  $I_Y = 2.5$  km and the variance  $\sigma_Y^2 = 0.2$ .

### Stochastic capture zones

When the new stochastic models of the clay and transmissivity layers are incorporated into the original model, the capture zones become stochastic functions too. Their probability distributions are inferred through MC analysis comprising 500 MC realizations.

Figure 5 shows capture zone probability distributions for the total catchment and the 25 year capture zone. Both plots show a considerable degree of uncertainty. For the 25 year capture zone, the probability level  $P = 1$  is rarely achieved. Interestingly, the probability distribution does not comprise a large zone in the centre where  $P$  is exactly 1, and a small zone near the edges where  $P$  decreases from 1 to 0, as seen in the previous section. The different large and small scale patterns in the plots may be caused by a combination of factors resulting from the drainage system and pumping regimes.

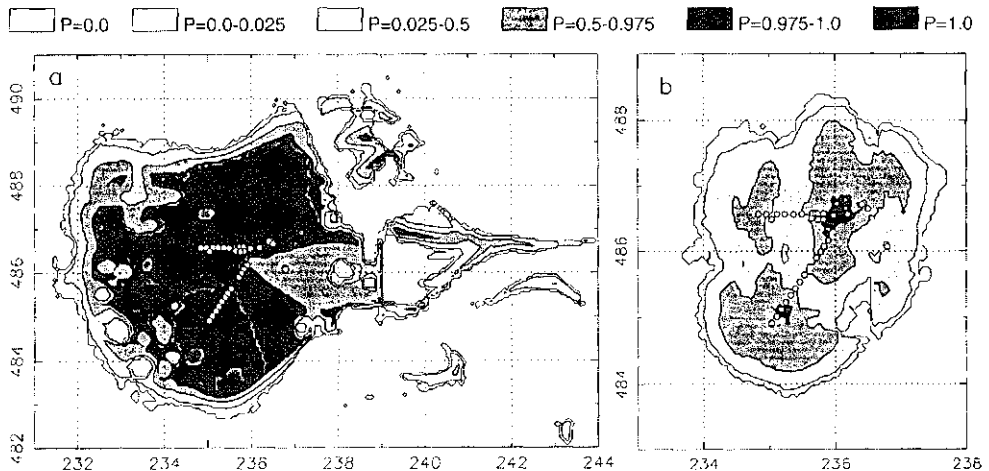


Fig. 5 Stochastic catchment (left) and 25 year capture zone (right), obtained with stochastic models of both the transmissivity of the production aquifer and the conductance of the clay layer.

## CONCLUSIONS

The present paper illustrates the value of the spatial stochastic MC method for characterizing the uncertainty in well capture zones due to aquifer heterogeneity. The results show how the properties of the production aquifer and any adjacent layers lead to a zone of uncertainty regarding the location of the well's capture zone. This naturally leads to the consideration of a risk-based approach where a well protection zone can be located at an agreed level of probability, e.g.  $0.025 < P < 0.975$ . Where site data is available, levels of uncertainty can be reduced by conditional simulation (Van Leeuwen *et al.*, 2000). Otherwise, estimates of aquifer heterogeneity can be used to enable this uncertainty to be incorporated in model applications.

## REFERENCES

- Broers, H. P., Hoogendoorn, J. H. & Houtman, H. (1994) Opbouw van het geohydrologische lagenmodel van REGIS/Digitale Grondwaterkaart, Deel I: Constructie van het lagenmodel, Deel II: Overzicht van gidslagen en gidsgrensvlakken (Structure of the hydrogeological layer model of REGIS/Digital ground water map, Part I: Construction of the layer model, Part II: Overview of model layers and model intersection layers). *Report no. OS 94-04A, NITG-TNO Dutch Institute for Applied Geoscience*.
- Franzetti, S. & Guadagnini, A. (1996) Probabilistic estimation of well catchments in heterogeneous aquifers. *J. Hydrol.* **174**, 149–171.
- Guadagnini, A. & Franzetti, S. (1999) Time-related capture zones for contaminants in randomly heterogeneous formations. *Ground Water* **37**, 253–260.
- Hocksema, R. J. & Kitanidis, P. K. (1985) Analysis of the spatial structure of properties of selected aquifers. *Wat. Resour. Res.* **21**(4), 563–572.
- Hoogendoorn, J. & Te Stroet, C. B. M. (1994) Optimalisatie waterbeheer Wierden/Wierdense veld (Optimization water management Wierden/Wierden field). *Report no. OS 94-14-B, TNO-GG Dutch Institute for Applied Geoscience*.
- Te Stroet, C. B. M. (1995) Calibration of stochastic groundwater flow models: estimation of noise statistics and model parameters. PhD Thesis, Delft University of Technology, Delft, The Netherlands.
- Van Leeuwen, M., Te Stroet, C. B. M., Butler, A. P. & Tompkins, J. A. (1998) Stochastic determination of well capture zones. *Wat. Resour. Res.* **34**(9), 2215–2223.
- Van Leeuwen, M., Te Stroet, C. B. M., Butler, A. P. & Tompkins, J. A. (1999) Stochastic determination of the Wierden (Netherlands) capture zones. *Ground Water* **37**(1), 8–17.
- Van Leeuwen, M., Butler, A. P., Te Stroet, C. B. M. & Tompkins, J. A. (2000) Stochastic determination of well capture zones conditioned on regular grids of transmissivity measurements. *Wat. Resour. Res.* **36**(4), 949–957.
- Varljen, M. D. & Shafer, J. M. (1991) Assessment of uncertainty in time-related capture zones using conditional simulation of hydraulic conductivity. *Ground Water* **29**, 737–748.